

Hauser et al.<sup>[7]</sup> and later extended to fractal dimensions by several groups.<sup>[8,9]</sup> Nevertheless, only little experimental evidence has been published to prove 1D energy transfer. In the strict sense, one-dimensionality can be understood as a transport along a line or at least along an isolated file. However, one-dimensionality in the 3D space of an object of, for example, cylindrical morphology can also mean that the net transport of the individual transfer steps goes along the *c* axis of the cylinder, that is, along a well-defined axis. We call this quasi-1D to avoid any confusion.

One way to try to realize the conditions in which quasi-1D transport of excitation energy should be favored is by using dye molecules in a crystalline host that consists of 1D channels. Panchromatic chromophore mixtures in an AlPO<sub>4-5</sub> molecular sieve show interesting luminescence properties.<sup>[10]</sup> We have shown that zeolite L, with its 1D channels, is a very versatile material with which to build artificial host–guest antenna systems.<sup>[11]</sup> The channels are occupied by energy-transporting dyes (donors, D) and energy-trapping dyes (acceptors, A); strongly luminescent dyes are usually selected. The energy-transfer process that occurs when an excited donor transports its excitation energy to an unexcited acceptor proceeds with a Förster-type mechanism and its rate constant  $k_{DA}$  can be expressed according to Equation (1), in which  $\phi_D$  and  $\tau_D$  are the

$$k_{DA} \propto \frac{\phi_D}{\tau_D} J_{DA} \frac{\kappa_{DA}^2}{R_{DA}^6} \quad (1)$$

fluorescence quantum yield and lifetime, respectively, of the donor,  $J_{DA}$  is the spectral overlap integral between the donor emission and the acceptor absorption spectra,  $\kappa_{DA}$  describes the relative orientation of the electronic transition moments, and  $R_{DA}$  is the distance between D and A.

$R_{DA}$  has a strong effect on the energy-transfer rate constant. It can be tuned, for example, by varying the loading of the dye molecules<sup>[12]</sup>, which changes the overall dye–dye distance. Another elegant way to study the distance dependence of the transfer of excitation energy is to introduce a spacer molecule between the donors and the acceptors to separate them locally, as illustrated in Figure 1. To realize this introduction, a defined quantity of acceptor molecules was first incorporated into the channels of zeolite L. In the second step, different quantities of spacer molecules were incorporated into the channels that already contained acceptor dyes, thus forming spacer layers of different thicknesses. In the third step, the same quantity of donor dyes was always added. As the conditions are such that the dyes cannot glide past each other, the crystal is divided into compartments in which the density of one dye is dominant. By selectively exciting the donor, the behavior of the excitation energy can be observed as it depends on the amount of spacer molecules and therefore on the distance  $R_{DA}$ . Is the transport of electronic excitation energy preferentially quasi-1D along the cylinder axis?

With the dye molecules listed in Scheme 1, we investigated three systems. Two systems have been synthesized according to Figure 1 A, in which Py<sup>+</sup> acts as donor and Ox<sup>+</sup> as acceptor. Owing to its favorable spectral properties and its

## Zeolites

DOI: 10.1002/ange.200500431

## Förster-Type Energy Transfer along a Specified Axis\*\*

Claudia Minkowski and Gion Calzaferri\*

Förster transfer of electronic excitation energy in 3D<sup>[1–3]</sup> and 2D<sup>[4,5]</sup> systems has been studied in many laboratories. Kuhn extended the Förster theory of long-range energy transfer in 3D systems to 2D and 1D systems.<sup>[6]</sup> The theory of the time dependence of this process in 1D and 2D cases was studied by

[\*] Dipl.-Chem. C. Minkowski, Prof. Dr. G. Calzaferri  
Department of Chemistry and Biochemistry  
University of Bern  
Freiestrasse 3, 3012 Bern (Switzerland)  
Fax: (+41) 31-631-39-94  
E-mail: gion.calzaferri@iac.unibe.ch

[\*\*] This work was supported by the Schweizerischer Nationalfonds zur Förderung der wissenschaftlichen Forschung NF 200020-105140/1 and NRP47 4047-57481. Zeolite L was synthesized by Dr. A. Khatyr and Dr. S. Megelski. Time-resolved measurements were carried out by K. Lutkouskaya.

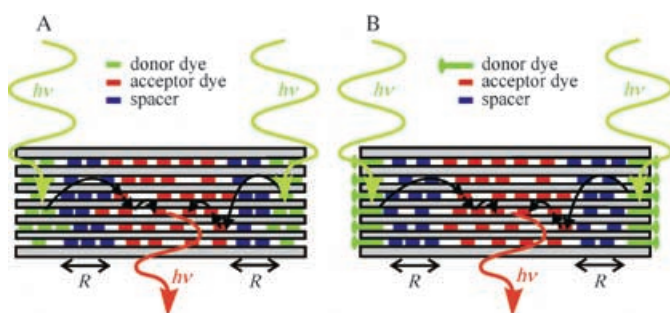
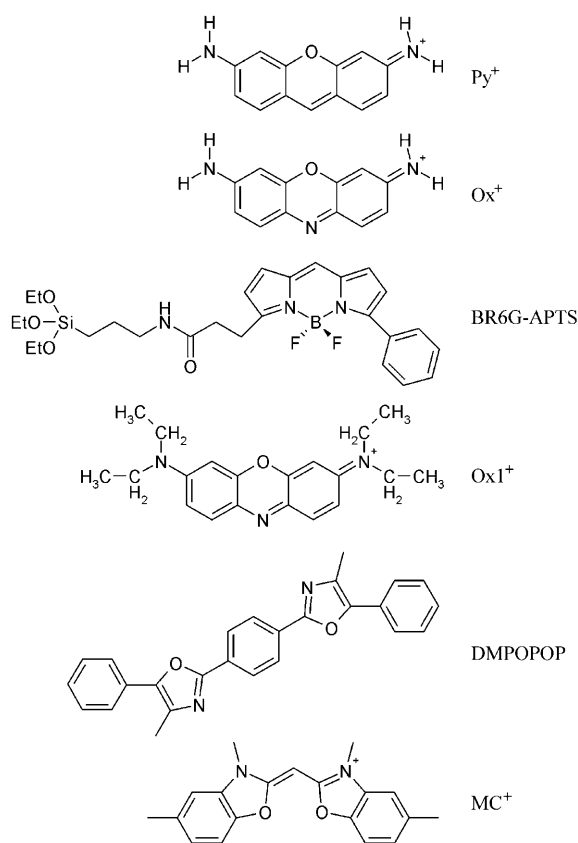


**Figure 1.** Schematic representation of zeolite L, which illustrates the parallel channels that run along the *c* axis of the crystal. The channels contain red-light-emitting dyes in the middle, followed by different amounts of spacer molecules (blue) that form spacer layers of different average thicknesses, and finally green-light-emitting donors at both ends. A) The donor–spacer and spacer–acceptor phase boundaries are diffuse. B) The donor dye is a stopper molecule with a tail that enters the channels but a head that is too large to enter. All donors are fixed at the same position and only the spacer–acceptor phase boundary is diffuse.



**Scheme 1.** Dyes used for the loading of zeolite L: Py<sup>+</sup> and BR6G-APTS (donors), Ox<sup>+</sup> and Ox1<sup>+</sup> (acceptors), and DMPOPOP and MC<sup>+</sup> (spacers).

high fluorescence quantum yields, this donor–acceptor pair exhibits a remarkable ability to transport excitation energy through Py<sup>+</sup> energy carriers to luminescent Ox<sup>+</sup> traps. The third system has been synthesized according to Figure 1B, in which BR6G-APTS acts as a “stopper” donor and Ox1<sup>+</sup> as the

acceptor. Specific attachment of the triethoxysilyl group of this stopper donor at the entrance of the channels was carried out according to a previous report.<sup>[13]</sup> The spacer molecules—in our case dyes as well—must be chosen so that they do not participate in the energy-transfer process; that is, they should not absorb in the spectral region where the donor is excited and they should not trap the energy from the donor. In the first and third systems, DMPOPOP was used as the spacer to give the antenna systems Py<sup>+</sup>/DMPOPOP/Ox<sup>+</sup>–zeolite L (**1**) and BR6G-APTS/DMPOPOP/Ox1<sup>+</sup>–zeolite L (**3**), whereas in the second system, MC<sup>+</sup> was used to give the antenna system Py<sup>+</sup>/MC<sup>+</sup>/Ox<sup>+</sup>–zeolite L (**2**). For **1** and **2**, zeolite L crystals of 840 nm length were used, whereas for **3**, the crystals were 300 nm long. The left column of Figure 2 shows the excitation and emission spectra of the individual dye molecules inserted into zeolite L.

For each of the three systems, a series of four samples were synthesized. The amount of donor and acceptor was kept constant, whereas the amount of spacer, namely DMPOPOP and MC<sup>+</sup>, was increased from samples 1 to 4 in each series. From the amount of spacer, the average number of spacer molecules per spacer layer (*n*) can be calculated. This value determines the mean distance between the donor and acceptor molecules. Emission spectra of the different samples were recorded. The donor was selectively excited and the spectra were scaled to the same height of the donor emission (Figure 2, right column). In all three systems, the first sample with the smallest spacer layer shows the highest acceptor fluorescence intensity. With an increasing number of spacer molecules per layer, less and less energy transfer occurs and thus the acceptor fluorescence intensity decreases.

The distance dependence of the probability *P* for Förster-type long-range energy transfer from an electronically excited donor to an acceptor can be simplified according to Equation (2). *R*<sub>0</sub> is the Förster radius; the exponent *α* is 6 for 3D

$$P = \frac{1}{1 + (R_{DA}/R_0)^\alpha} \quad (2)$$

systems,<sup>[1]</sup> 4 for 2D systems,<sup>[3]</sup> and 2 for 1D systems.<sup>[6]</sup> We do not have direct access to the mean value of *R*<sub>DA</sub> (*R*<sub>DA</sub>). However, the average number of spacer molecules per spacer layer is proportional to this mean distance. Therefore, we have plotted the acceptor fluorescence intensity versus 1/(1+*n*<sup>*α*</sup>) for different values of *α* ranging from 6 to 1 and we found that all data obey an *α* = 2 dependence (Figure 3). *I*<sub>rel</sub> does not go to zero at (1+*n*<sup>2</sup>)<sup>−1</sup> → 0 as the acceptor absorbs to a small degree at the wavelength of excitation. The numbers of spacer molecules in these experiments are reported in Table 1.

It is not possible to estimate *R*<sub>DA</sub> by multiplying the number of spacer molecules by their lengths (2.02 nm for DMPOPOP and 1.48 nm for MC) as energy transfer is not restricted to individual channels (see Figure 1 and Figure 4). The spectral overlap integrals and the corresponding Förster radii in parenthesis, which are calculated for a numerically estimated *κ*<sub>DA</sub><sup>2</sup> value of about 1 and an estimated refractive index of 1.4, are *J*<sub>Py<sup>+</sup>,Ox<sup>+</sup></sub> = 2.3 × 10<sup>−10</sup> cm<sup>6</sup> mol<sup>−1</sup> (6.1 nm) and *J*<sub>BR6G-APTS,Ox1<sup>+</sup></sub> = 5.6 × 10<sup>−10</sup> cm<sup>6</sup> mol<sup>−1</sup> (7.1 nm).<sup>[14]</sup>

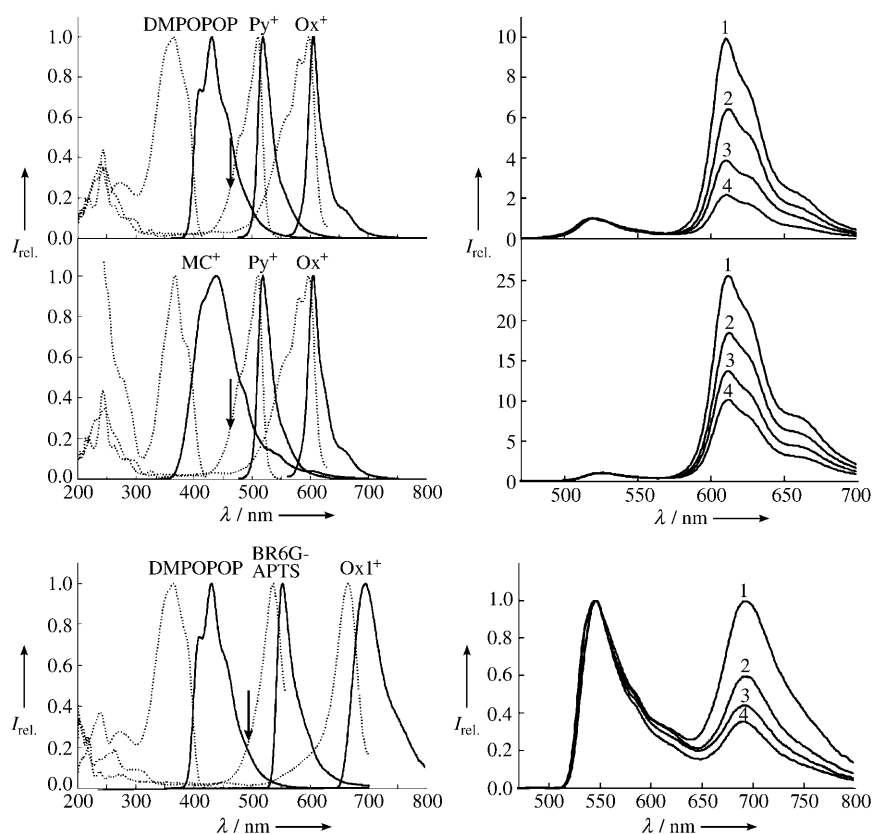


**Figure 2.** Left: Excitation (dotted lines) and emission (solid lines) spectra of the applied dye molecules. Right: Fluorescence spectra (scaled to the maximum of the donor emission) for **1** (top), **2** (middle), and **3** (bottom), with different amount of spacer, after selective excitation of the donor at the wavelengths indicated by the arrows in the left spectra. Average number of spacer molecules per spacer layer ( $n$ ) for 1–4: top: 8.5, 11, 16, 22.5; middle: 15, 17.5, 24, 36.5; bottom: 2.7, 4, 6, 10.

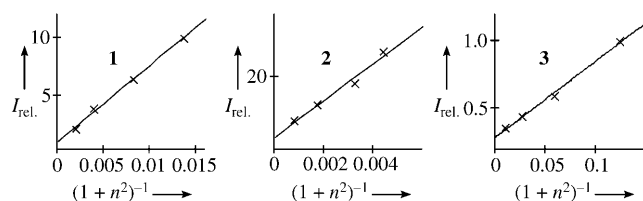


**Figure 3.** Intensities  $I_{\text{rel}}$  of the acceptor fluorescence versus the averaged number of spacer molecules per spacer layer ( $n$ ) in **1**–**3** confirming the value of  $\alpha = 2$ .

**Table 1:** Values of  $n$  and the relative luminescence intensities of the acceptors for all the samples studied.

Sample	<b>1</b>		<b>2</b>		<b>3</b>	
	$n$	$I_{\text{rel}}$	$n$	$I_{\text{rel}}$	$n$	$I_{\text{rel}}$
1	8.5	9.92	15	25.55	2.7	0.99
2	11	6.4	17.5	18.44	4	0.59
3	16	3.86	24	13.70	6	0.44
4	22.5	2.15	36.5	11.10	10	0.35

One difficulty in analyzing the data in Figure 3 and Table 1 according to Equation (2) is that  $n$  is proportional but not equal to  $(R_{\text{DA}}/R_0)$ . We can write this as follows  $(R_{\text{DA}}/R_0) =$

$cn$ , in which  $c$  is a constant. What we know is that  $R_{\text{DA}}$  must be in the order of  $R_0$  because the amount of energy transfer is substantial in all samples.  $R_0$  is the radius at which the energy-transfer probability is 50%. From this we can estimate that  $c$  is less than 1 but we also know that  $R_{\text{DA}}$  cannot be smaller than the distance between the centers of two channels, which is 1.84 nm; thus  $1 > c > 0.2$ . With this range for  $c$ , it is easy to verify numerically that plotting the relative intensities versus  $1/(1+n^\alpha)$  allows us to discriminate between different  $\alpha$  values and only  $\alpha = 2$  is consistent with the measurements for all three materials.

In **1** and **2**, the donors are dyes that also enter the channels. The dyes cannot glide past each other within a channel, but their positions can overlap with neighboring channels to reveal a staggered profile of the phase boundaries (see Figure 1 and Figure 4). Replacing the donors with stopper molecules as in **3**, which have a tail that can enter the channel but a head too large to enter, results in a less-diffuse phase boundary. In this case, all stopper donors are fixed at the same position and only one staggered phase boundary from the spacer to the acceptor remains.

We report time-resolved data for the luminescence decay of the donor for each of the four samples of **1** and **2** (Table 2). The data were evaluated with a biexponential fit with lifetimes  $\tau_1$  and  $\tau_2$ , with the factor  $f_1$  indicating the number of photons that decay with lifetime  $\tau_1$ . A  $\text{Py}^+$ -zeolite L sample with a loading of 0.02 decays with a mean lifetime  $\langle \tau \rangle$  of 2.4 ns.<sup>[15]</sup> The decay of the donor in sample 4 of **1** is much faster than that of  $\text{Py}^+$ -zeolite L due to energy transfer, and the rate of decay increases from sample 4 to 1. This observation is in agreement with the steady-state emission spectra of these samples. The

**Table 2:** Decay [ns] of the luminescence of donor  $\text{Py}^+$  in **1** and **2**.<sup>[a]</sup>

System	Sample	$\langle \tau \rangle$	$\tau_1$	$\tau_2$	$f_1$
$\text{Py}^+$ -zeolite L		2.4			
<b>1</b>	1	0.13	0.007	1.26	0.90
	2	0.27	0.105	2.00	0.91
	3	0.45	0.11	1.43	0.75
	4	0.89	0.24	2.16	0.66
<b>2</b>	1	0.21	0.05	2.96	0.95
	2	0.22	0.04	3.07	0.94
	3	0.25	0.04	2.47	0.91
	4	0.29	0.04	2.75	0.91

[a] Excitation at 465 nm; detection at 520 nm.

luminescence decay of the donor of **2** is already very fast for sample 4 and increases slightly from sample 4 to 1. As can be observed in the steady-state spectra (Figure 2), the acceptor fluorescence intensities of the samples of **2** are higher than those of **1**.

We have added some theoretical reasoning to explain better the system. First we focus on the distribution of the dye molecules at the phase boundaries. We can assume a uniform distribution of the dyes, as proposed by the results of a Monte Carlo calculation.<sup>[15]</sup> Figure 4A reveals the staggered profile

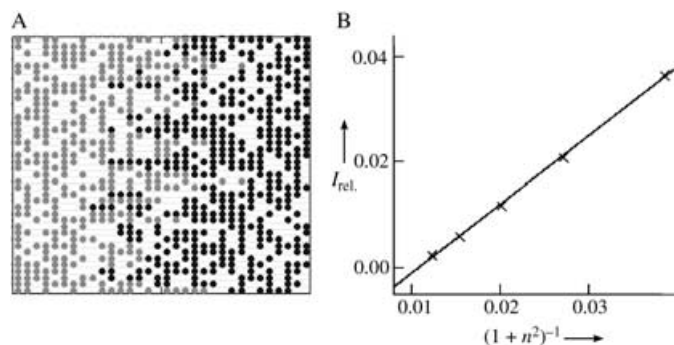


**Figure 4.** A) Simulated image of a zeolite L crystal containing 40 channels with each channel containing 32 sites, obtained by a Monte Carlo calculation; it illustrates the phase boundary. The sites are randomly filled with one type of dye molecule (dark dots), while after virtually sealing the right channel entrances another type of dye (light dots) was added from the left side. The overall occupation of both dye molecules per available site is 60%. The phase boundaries extend over about 10 sites. B) Calculated intensities of  $I_{rel}$  of the acceptor fluorescence versus averaged number of spacer molecules ( $n$ ) between donor and acceptor for  $\alpha=2$ .

of the borders. Figure 4B shows the same  $\alpha=2$  dependence for a calculated system in which the energy-migration and energy-transfer steps are described as a random walk by means of Markov chains.<sup>[16]</sup>

The experimental data reported in Figures 2 and 3, and in Tables 1 and 2 can only be understood in terms of the long-range energy transfer of Förster. A trivial mechanism would not cause a shortening of the lifetime of the donor luminescence. There would also be no or a much weaker dependence on distance for the efficiency of the energy transfer because the change in distances is more than one order of magnitude smaller than the wavelength of the light. We found that varying  $n$  has a strong effect on the rate of energy transfer, as can be observed in the fluorescence intensities of the acceptors in samples in which the number of spacer molecules is different. This can also be observed in the time-resolved measurements in which the mean lifetimes ( $\tau$ ) of the donor increase with an increase in  $n$  due to a decrease in energy transfer to the acceptor. System **2** has a much shorter ( $\tau$ ) value than **1**, although the number of spacer molecules per layer is higher for **2** than for **1**. Thus we assume that  $MC^+$  is more packed than DMPOPOP.

The correlation of the acceptor fluorescence intensity versus the number of spacer molecules per layer leads to a linearization at  $1/(1+n^2)$ . The same result is observed in the

theoretical simulation. The individual transfer steps can also occur to a neighboring channel, but the statistical mean of the energy transfer in the dye-loaded zeolite L crystals is directed along the  $c$  axis of the cylinder. Hence, the transport of electronic excitation energy in all three systems is quasi-1D. This observation is of considerable interest for the development of highly anisotropic optoelectronic devices, some of which have already been proposed.<sup>[11]</sup>

## Experimental Section

Zeolite L crystals were synthesized and characterized as described previously.<sup>[17]</sup> The potassium-exchanged form was used, which had an average crystal length of 840 nm for **1** and **2**, and 300 nm for **3**.  $Py^+$  and  $Ox^+$  were synthesized and purified according to a reported procedure.<sup>[18]</sup> DMPOPOP (Fluka),  $MC^+$  (CIBA-GEIGY AG), and Cryptofix 222 (Fluka) were used as received. BR6G-APTS was made by substituting BODIPY-RG6 (succinimidyl ester of 4,4-difluoro-5-phenyl-4-bora-3a,4a-diaza-s-indacene-3-propionic acid, Molecular Probes), with (3-aminopropyl)triethoxysilane (Fluka). The two compounds were dissolved in  $CH_2Cl_2$  and stirred for 1 h, the  $CH_2Cl_2$  was removed by evaporation, and the resulting precipitate was washed twice with cyclohexane.<sup>[19]</sup>

**1:** Zeolite L was suspended in water and sonicated for 20 min to avoid aggregation of the crystals. An aqueous solution containing the required amount of  $Ox^+$  was added and the resulting mixture was heated at reflux for 7 h. The  $Ox^+$ -loaded zeolite L crystals were washed with methanol to remove the  $Ox^+$  from the surface. Insertion of DMPOPOP:<sup>[11]</sup>  $Ox^+$ -loaded zeolite L crystals were transferred into a glass ampoule and dehydrated under vacuum ( $3 \times 10^{-2}$  mbar) at 80 °C for 24 h to empty the adsorption sites in the channels. The required amount of DMPOPOP was added and the ampoule was sealed. The sealed ampoule was heated in a rotating furnace at 150 °C for 6 days, after which the DMPOPOP/ $Ox^+$ -zeolite L crystals were washed with  $n$ -butanol and rehydrated in an exsiccator that contained a saturated solution of potassium acetate. Incorporation of  $Py^+$ : The DMPOPOP/ $Ox^+$ -zeolite L was suspended in water, and an aqueous solution of  $Py^+$  was added and the mixture heated at reflux for 30 min. Compound **1** was washed again with methanol to remove dye molecules on the crystal surface.

**2:** First step as described for **1**. The incorporation of  $MC^+$  was more involved and was carried out stepwise to obtain higher loadings:  $Ox^+$ -Zeolite L was suspended in a mixture of  $n$ -butanol and water (1:10) and sonicated for 20 min. A solution of  $MC^+$  in the same  $n$ -butanol/water mixture was added to the suspension, which also contained an excess of Cryptofix 222.<sup>[18]</sup> The mixture was then heated at 65 °C for over 48 h to obtain a loading of about 40 to 50 % of the preset amount of  $MC^+$ . The  $MC^+$ / $Ox^+$ -zeolite L crystals were then washed with methanol and the insertion was repeated up to four times.  $MC^+$ / $Ox^+$ -zeolite L was suspended in water and an aqueous solution containing the required amount of  $Py^+$  was added; this mixture was heated at reflux for 30 min. Compound **2** was washed again with methanol.

**3:** Zeolite L was suspended in toluene and sonicated for 20 min. A solution of  $Ox1^+$  in toluene and an excess of Cryptofix 222 was added and the resulting mixture was heated at 65 °C for 7 h. The  $Ox1^+$ -loaded zeolite L crystals were washed with methanol. Insertion of DMPOPOP as outlined for **1**. BR6G-APTS was added by dissolving the DMPOPOP/ $Ox1^+$ -zeolite L in  $Cl_2CH_2$  and adding the required amount of the stopper molecule. The mixture was sonicated for 30 min and stirred at room temperature for 20 h.<sup>[13]</sup> Compound **3** was dried, dissolved in  $n$ -hexane, heated at reflux for 2 h, and again washed with methanol. The amount of dye molecules inside the channels was determined by destroying the zeolite framework with HF: A solution of HF (8 %, 100  $\mu$ L) was added to a solution of  $n$ -butanol (3.9 mL) containing the dye-loaded zeolite L (1 mg) in a



polypropylene tube and this mixture was sonicated for 5 min. The amount of dye entering the solution was determined by UV/Vis spectroscopy.<sup>[12]</sup>

Thin-layer preparation: Dye-loaded zeolite L (100 µL) suspended in *n*-butanol ( $\approx 1$  mg in 300 µL) was dropped onto a quartz plate ( $\varnothing 1.6$  cm) and the solvent was evaporated in air. The quartz plate was then covered with a Petri dish. Emission and excitation spectra were recorded on a Perkin Elmer LS 50B luminescence photometer. Compounds **1** and **2** were excited at 460 nm with a cut-off filter at 490 nm; compound **3** was excited at 490 nm with a cut-off filter at 510 nm. The samples were measured as thin layers on quartz. Time-resolved measurements were carried out according to a reported procedure.<sup>[15]</sup> Samples were excited at 465 nm and detected at 520 nm; slit widths = 4 nm. Optical fluorescence microscopy images were carried out on an Olympus BX 60 device equipped with a Kappa CF 20 DCX Air K2 CCD camera.<sup>[11]</sup>

Received: February 4, 2005

Revised: June 7, 2005

Published online: July 25, 2005

**Keywords:** fluorescence · FRET (fluorescence resonant energy transfer) · host–guest systems · supramolecular chemistry · zeolites

- [14] S. Megelski, A. Lieb, M. Pauchard, A. Drechsler, S. Glaus, C. Debus, A. J. Meixner, G. Calzaferri, *J. Phys. Chem. B* **2001**, *105*, 25.
- [15] M. M. Yatskou, M. Meyer, S. Huber, M. Pfenniger, G. Calzaferri, *ChemPhysChem* **2003**, *4*, 567.
- [16] N. Gfeller, G. Calzaferri, *J. Phys. Chem. B* **1997**, *101*, 1396.
- [17] A. Zabala Ruiz, D. Brühwiler, G. Calzaferri, *Monatsh. Chem.* **2005**, *136*, 77.
- [18] H. Maas, A. Khatyr, G. Calzaferri, *Microporous Mesoporous Mater.* **2003**, *65*, 233.
- [19] S. Huber, G. Calzaferri, *Angew. Chem.* **2004**, *116*, 6906; *Angew. Chem. Int. Ed.* **2004**, *43*, 6738.

- [1] T. Förster, *Fluoreszenz organischer Verbindungen*, Vandenboeck & Ruprecht, Göttingen, **1951**.
- [2] D. L. Andrews, A. A. Demidov, *Resonance Energy Transfer*, Wiley, New York, **1999**.
- [3] a) B. Valeur, *Molecular Fluorescence*, Wiley-VCH, Weinheim, **2002**; b) J. R. Lakowicz, *Principles of Fluorescence Spectroscopy*, 2nd ed., Kluwer Academic-Plenum, New York, **1999**; c) X. F. Wang, B. Herman, *Fluorescence Imaging Spectroscopy and Microscopy*, Wiley, New York, **1996**.
- [4] a) H. Bücher, K. H. Drexhage, M. Fleck, H. Kuhn, D. Möbius, F. P. Schäfer, J. Sondermann, W. Sperling, P. Tillmann, J. Wiegand, *Mol. Cryst.* **1967**, *2*, 199; b) H. Kuhn, D. Möbius, *Physical Methods of Chemistry, Vol. IXB* (Eds.: B. W. Rossiter, R. C. Baetzold), Wiley, New York, **1993**, pp. 375–542.
- [5] a) G. Zumofen, A. Blumen, *J. Chem. Phys.* **1982**, *76*, 3713; b) P. Anfinrud, R. L. Crackel, W. S. Struve, *J. Phys. Chem.* **1984**, *88*, 5873; c) N. Tamai, T. Yamazaki, I. Yamazaki, *J. Phys. Chem.* **1987**, *91*, 841.
- [6] H. Kuhn, *J. Chem. Phys.* **1970**, *53*, 101.
- [7] M. Hauser, U. K. A. Klein, U. Gösele, *Z. Phys. Chem. Neue Folge* **1976**, *101*, 255.
- [8] a) Z. Tang, B. Ozturk, Y. Wang, N. A. Kotov, *J. Phys. Chem. B* **2004**, *108*, 6927; b) D. Sendor, M. Hilder, T. Juestel, P. C. Junk, U. H. Kynast, *New J. Chem.* **2003**, *27*, 1070; c) B. Maliwal, J. Kusba, J. R. Lakowicz, *SPIE* **1992**, *1640*, 586; d) J. Grabowska, K. Sienicki, *Chem. Phys.* **1995**, *192*, 89.
- [9] a) J. Klafter, J. M. Drake, *Molecular Dynamics in Restricted Geometries*, Wiley, New York, **1989**; b) S. E. Webber, *Chem. Rev.* **1990**, *90*, 1469; c) J. Klafter, A. Blumen, *J. Chem. Phys.* **1984**, *80*, 875; d) P. Levitz, J. M. Drake, *Phys. Rev. Lett.* **1987**, *58*, 686; e) J. P. S. Farinha, J. G. Spiro, M. A. Winnik, *J. Phys. Chem. B* **2001**, *105*, 4879.
- [10] M. Ganschow, C. Hellriegel, E. Kneuper, M. Wark, C. Thiel, G. Schulz-Ekloff, C. Bräuchle, D. Wöhrle, *Adv. Funct. Mater.* **2004**, *14*, 269.
- [11] G. Calzaferri, S. Huber, H. Maas, C. Minkowski, *Angew. Chem.* **2003**, *115*, 3860; *Angew. Chem. Int. Ed.* **2003**, *42*, 3732.
- [12] S. Megelski, G. Calzaferri, *Adv. Funct. Mater.* **2001**, *11*, 277.
- [13] T. Ban, D. Brühwiler, G. Calzaferri, *J. Phys. Chem. B* **2004**, *108*, 16348.